

RESEARCH ARTICLE

Open Access

# Intracellular pH regulation: characterization and functional investigation of H<sup>+</sup> transporters in *Stylophora pistillata*



Laura Capasso<sup>1,2</sup>, Philippe Ganot<sup>1</sup>, Víctor Planas-Bielsa<sup>1</sup>, Sylvie Tambutté<sup>1</sup> and Didier Zoccola<sup>1\*</sup> 

## Abstract

**Background:** Reef-building corals regularly experience changes in intra- and extracellular H<sup>+</sup> concentrations ([H<sup>+</sup>]) due to physiological and environmental processes. Stringent control of [H<sup>+</sup>] is required to maintain the homeostatic acid-base balance in coral cells and is achieved through the regulation of intracellular pH (pH<sub>i</sub>). This task is especially challenging for reef-building corals that share an endosymbiotic relationship with photosynthetic dinoflagellates (family Symbiodinaceae), which significantly affect the pH<sub>i</sub> of coral cells. Despite their importance, the pH regulatory proteins involved in the homeostatic acid-base balance have been scarcely investigated in corals. Here, we report in the coral *Stylophora pistillata* a full characterization of the genomic structure, domain topology and phylogeny of three major H<sup>+</sup> transporter families that are known to play a role in the intracellular pH regulation of animal cells; we investigated their tissue-specific expression patterns and assessed the effect of seawater acidification on their expression levels.

**Results:** We identified members of the Na<sup>+</sup>/H<sup>+</sup> exchanger (SLC9), vacuolar-type electrogenic H<sup>+</sup>-ATP hydrolase (V-ATPase) and voltage-gated proton channel (H<sub>v</sub>CN) families in the genome and transcriptome of *S. pistillata*. In addition, we identified a novel member of the H<sub>v</sub>CN gene family in the cnidarian subclass Hexacorallia that has not been previously described in any species. We also identified key residues that contribute to H<sup>+</sup> transporter substrate specificity, protein function and regulation. Last, we demonstrated that some of these proteins have different tissue expression patterns, and most are unaffected by exposure to seawater acidification.

**Conclusions:** In this study, we provide the first characterization of H<sup>+</sup> transporters that might contribute to the homeostatic acid-base balance in coral cells. This work will enrich the knowledge of the basic aspects of coral biology and has important implications for our understanding of how corals regulate their intracellular environment.

**Keywords:** H<sup>+</sup> transport, Reef-building corals, pH regulation, Gene expression, Ocean acidification

\* Correspondence: [zoccola@centrescientifique.mc](mailto:zoccola@centrescientifique.mc)

<sup>1</sup>Centre Scientifique de Monaco, 8 quai Antoine 1er, 98000 Monaco, Monaco

Full list of author information is available at the end of the article



© The Author(s). 2021 **Open Access** This article is licensed under a Creative Commons Attribution 4.0 International License, which permits use, sharing, adaptation, distribution and reproduction in any medium or format, as long as you give appropriate credit to the original author(s) and the source, provide a link to the Creative Commons licence, and indicate if changes were made. The images or other third party material in this article are included in the article's Creative Commons licence, unless indicated otherwise in a credit line to the material. If material is not included in the article's Creative Commons licence and your intended use is not permitted by statutory regulation or exceeds the permitted use, you will need to obtain permission directly from the copyright holder. To view a copy of this licence, visit <http://creativecommons.org/licenses/by/4.0/>. The Creative Commons Public Domain Dedication waiver (<http://creativecommons.org/publicdomain/zero/1.0/>) applies to the data made available in this article, unless otherwise stated in a credit line to the data.

## Background

Coral reefs are among the most valuable ecosystems on earth, harbouring more than one-third of ocean biodiversity and providing economic benefits to tropical coastal nations worldwide [1]. Scleractinian corals are the major constructors of coral reefs, and most of them have mutualistic relationships with endosymbiotic dinoflagellate (family Symbiodinaceae)-symbiotic corals that provide photosynthetic products that support coral metabolism, growth and reproduction [2–4]. Despite their environmental significance, scleractinian corals face many challenges to their survival, including ocean acidification (OA), as a result of rising carbon dioxide levels in the atmosphere [5]. The effects of OA on the coral calcification rate and skeletal growth, including varied species-specific responses, have been previously documented [6–9]. Most of these effects have been proposed to be linked to acid-base regulatory processes and to lead to altered ionic concentration and energy expenditure and allocation [10]. Although acid-base regulatory processes might modulate physiological responses to OA, the pH regulatory proteins responsible for acid-base homeostasis are still poorly characterized in corals.

Corals are diploblastic animals, which means that they are made of two cell layers, an ectoderm and an endoderm, separated by a layer of mesoglea. Both ectoderm and endoderm are present in the oral and aboral tissue located on either side of the gastrovascular cavity (coelenteron) [11]. Each tissue possesses several cell subtypes that achieve acid-base homeostasis via pH regulation within physiological boundaries compatible with cell functioning [12]. This is especially challenging for symbiotic corals, as photosynthesis significantly increases the pH of coral cells [13, 14]. Symbiotic corals can experience large variations in extracellular pH ( $\text{pH}_e$ ) due to physiological (e.g., respiration, calcification and photosynthesis) and environmental (e.g., metabolism of reef-associated organisms, tides, water flow, upwelling and ocean acidification) factors. For example, symbiont photosynthesis and respiration of both the host and symbiont drive wide  $\text{pH}_e$  variations (from pH 8.5 to 6) in the internal fluid of the coelenteron [13–18], and exposure to acidified seawater decreases the  $\text{pH}_e$  in the extracellular calcifying medium (ECM) [9], where calcification occurs. These  $\text{pH}_e$  variations can also have an impact on the regulation of intracellular pH ( $\text{pH}_i$ ). For example, decreases in the  $\text{pH}_e$  of the ECM (from 8.3 to 7.8) under acidified seawater conditions affect the  $\text{pH}_i$  of calciblastic cells. Despite these variations, coral cells are able to maintain their  $\text{pH}_i$  within narrow limits (7.1–7.4) [9], showing that corals possess efficient  $\text{pH}_i$  regulatory mechanisms that account for this stability.

Under  $\text{pH}_i$  stress, an appropriate response depends on the ability to sense acid-base disturbances and react

through acid-base transport mechanisms [19]. Over the previous years, a number of acid-base cellular sensors, e.g., the acid-base sensing enzyme soluble adenylyl cyclase (sAC), and transport proteins have been proposed in corals on the basis of those characterized in vertebrates [20–22]. Acid-base transport proteins, which control  $\text{pH}_i$  regulation, fall into two groups, namely,  $\text{HCO}_3^-$  (solute carrier-SLC transporter family 4 and 26) and  $\text{H}^+$  membrane transporters [23]. Based on the energy source used for  $\text{H}^+$  extrusion,  $\text{H}^+$  membrane transporters can be further divided into transporters, pumps and channels. Transporters can move  $\text{H}^+$  against their electrochemical gradient by coupling  $\text{H}^+$  transport with pre-existing ion gradients as an energy source. This group includes the SLC9 family, also known as  $\text{Na}^+/\text{H}^+$  exchangers, which harness the electrochemical gradient of  $\text{Na}^+$  maintained by  $\text{Na}^+/\text{K}^+$ -ATPase [24]. The SLC9 family can be further divided into three subfamilies: subfamily A 1–9 (cation proton antiporter 1, CPA1), subfamily B 1–2 (cation proton antiporter 2, CPA2) and subfamily C 1–2 (Na-transporting carboxylic acid decarboxylase, NaT-DC) [25]. The second group of  $\text{H}^+$  membrane transporters in charge of  $\text{pH}_i$  regulation includes  $\text{H}^+$  pumps that allow  $\text{H}^+$  to move against its concentration gradient by coupling  $\text{H}^+$  transport to ATP hydrolysis. Vacuolar-type electrogenic  $\text{H}^+$ -ATP hydrolases (V-ATPases), which transport  $\text{H}^+$  via  $\text{V}_0$  V-ATPase subunit-a [26], and plasma membrane  $\text{Ca}^{+2}$ -ATPase (PMCA), which extrudes  $\text{Ca}^{+2}$  in exchange for  $\text{H}^+$  [19, 27, 28], belong to this group. Although some studies claim that  $\text{pH}_i$  regulation is not the primary role of these  $\text{H}^+$  pumps in most mammalian cells [19], others have suggested the opposite [29–32]. Members of the last group, the  $\text{H}^+$  channels, allow  $\text{H}^+$  to passively diffuse down its electrochemical gradient whenever the regulatory gate is open and includes voltage-gated proton channels ( $\text{H}_v\text{CN}$ ) [33, 34].

Despite their fundamental importance in  $\text{pH}_i$  regulation, the investigation of these  $\text{H}^+$  transporters is incomplete and includes only a limited number of marine species. For example, SLC9 and V-ATPase proteins have been identified in the transcriptome of calcifying primary mesenchymal cells of the sea urchin [35] and in the gills of fishes, where they are believed to play a role in acid-base regulation of the branchial epithelium [36, 37]. In addition, in white shrimp (*Litopenaeus vannamei*), squid (*Sepioteuthis lessoniana*), and sea anemone (*Anemonia viridis*), SLC9 has been shown to play a role in the response to low-pH stress [38–40]. In corals, among the acid-base transport proteins in charge of  $\text{pH}_i$  regulation, only  $\text{HCO}_3^-$  transporters have been characterized [20], whereas information regarding  $\text{H}^+$  membrane transporters is limited to  $\text{Ca}^{+2}$ -ATPase [41] and  $\text{V}_1$  V-ATPase subunit B [42].

In the present study, we provide a full characterization of the genomic structure, domain topology and phylogeny of the principal  $H^+$  transporters that might be involved in the intracellular pH regulation and maintenance of cellular physiological homeostasis in the symbiotic coral *Stylophora pistillata*. These transporters include  $Na^+/H^+$  exchangers, which are ion transporters that concurrently transport  $Na^+$  into the cell and  $H^+$  out of the cell; voltage-gated  $H^+$  channels ( $H_vCN$ ), which represent a specific subset of proton channels that have voltage- and time-dependent gating and thus only open to extrude  $H^+$  from the cell; and  $V_0$  V-ATPase subunit-a, which connects the two portions ( $V_0$  and  $V_1$ ) of the multi-subunit enzyme V-ATPase and is crucial for proton transport [19, 30, 43–45]. Furthermore, we characterized the gene expression patterns of  $H^+$  transporters to determine whether they are differentially expressed in coral tissues, and we discussed their potential physiological roles. In addition, we investigated the molecular response of *S. pistillata* to ocean acidification by assessing the effect of external seawater acidification on the levels of  $H^+$  transporter expression after 1 week and 1 year of exposure.

## Results

### Candidate $Na^+-H^+$ exchanger (SLC9) in *S. pistillata*: gene structure, amino acid sequence and phylogenetic analysis

We identified genes homologous to human *SLC9* in the genome and transcriptome of *S. pistillata* [46, 47]. Phylogenetic analysis of *S. pistillata* SLC9 proteins (spiSLC9) with functionally characterized SLC9 in humans allowed us to group the corresponding *S. pistillata* genes within three subfamilies, namely, subfamilies A, B and C (Fig. 1). Members of subfamily A are distributed in two different clusters (plasma membrane and organelle) that contain plasma membrane and organelle homologs, respectively. In addition, organelle homologs include two distinct branches (A8 and A6/7). Of the seven *SLC9* genes identified in *S. pistillata*, four belong to subfamily A (the NHE subfamily), one (*spiSLC9A1*) is a plasma membrane homolog, two (*spiSLC9A6* and *spiSLC9A7*) are A6/7 organelle homologs; one (*spiSLC9A8*) is an A8 organelle homolog; two (*spiSLC9B1* and *spiSLC9B2*) belong to subfamily B (the NHA subfamily); and one (*spiSLC9C*) belongs to subfamily C (the mammalian sperm NHE-like subfamily). The gene and transcript information of SLC9 family members is given in Additional files 1 and 2.

The exchange domain of spiSLC9s is predicted to have 8 to 12 transmembrane segments (TMs) (Additional file 3), which display sequence conservation in contrast to the higher variability observed at the N-termini and C-termini of the proteins. Sequence comparison of spiSLC9s showed similarities between members of the same subfamily, and

the percentages of similarity and identity varied for each subfamily. For members of subfamily A, the percentage of similarity varies between 50 and 57% (sharing 35% identity). However, members of subfamily B share 78% similarity (sharing 62% identity). spiSLC9 proteins also exhibit similarity with hSLC9s: spiSLC9A has 42–55% identity and 60–71% similarity to hSLC9A; spiSLC9B has 43–47% identity and 61–66% similarity to hSLC9B; and spiSLC9C has 26% identity and 50% similarity to hSLC9C. In addition, spiSLC9s possess conserved features with hSLC9s, including residues related to  $Na^+/H^+$  exchanger activity, such as F161, P167–168, R440 and G455–456, for members of subfamily A (Additional file 4); glycine zipper sequences (SLC9B1-GZ1: 275–283; SLC9B2-GZ1: 184–192; GZ2: 210–216; GZ3: 263–271) for members of subfamily B (Additional file 5); and a conserved voltage-sensing domain (VSD) composed of four transmembrane segments S1–S4 and a cyclic nucleotide-binding domain (CNBD) for members of subfamily C (Additional file 6).

Regarding post-translational modifications, several phosphorylation and N-glycosylation sites were predicted for spiSLC9s (Additional file 7).

### Candidate $V_0$ V-ATPase subunit-a in *S. pistillata*: gene structure, amino acid sequence and phylogenetic analysis

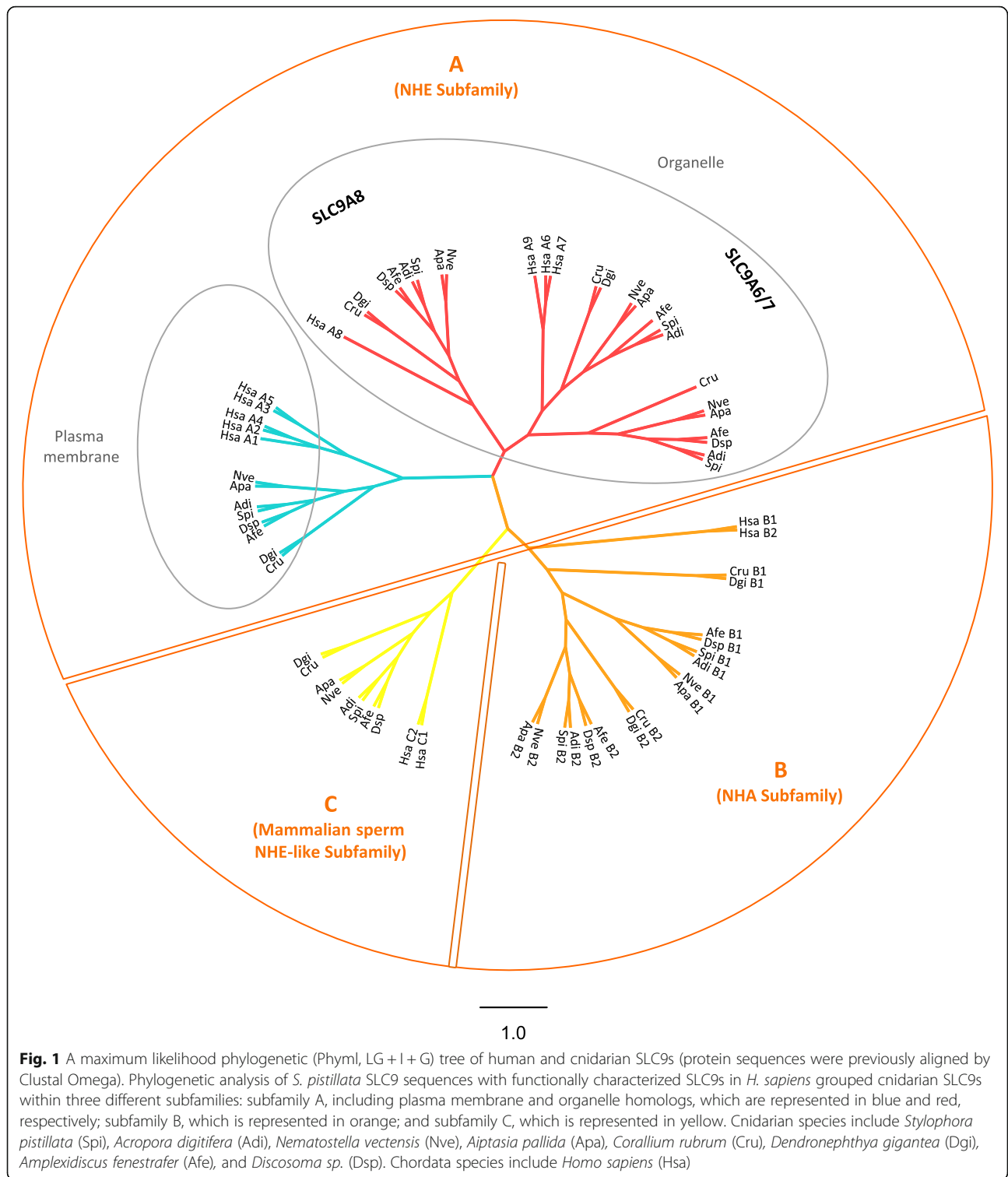
As previously described for *spiSLC9*, we identified one gene homologous to human  $V_0$  V-ATPase subunit-a in the genome and transcriptome of *S. pistillata*. The gene and transcript information of the  $V_0$  V-ATPase subunit-a gene is given in Fig. 2a and Additional file 2. *spiV\_0* V-ATPase subunit-a exists in four splice variants and is one of the 14 subunits composing the spiV-ATPase (Additional file 8).

The spiV<sub>0</sub> V-ATPase subunit-a protein has six predicted TMs (Additional file 3) and exhibits similarity to human homologs (44–64% similarity and 59–76% identity). Several residues (Fig. 2b) are conserved between spiV<sub>0</sub> V-ATPase and hV<sub>0</sub> V-ATPase, such as R735, L739, H743, E789, L746, R799 and V803. Regarding post-translational modifications, several phosphorylation and N-glycosylation sites were predicted for spiV<sub>0</sub> V-ATPase subunit-a (Additional file 7).

As previously described, we identified putative  $V_0$  V-ATPase subunit-a homologs in other species (Fig. 3).

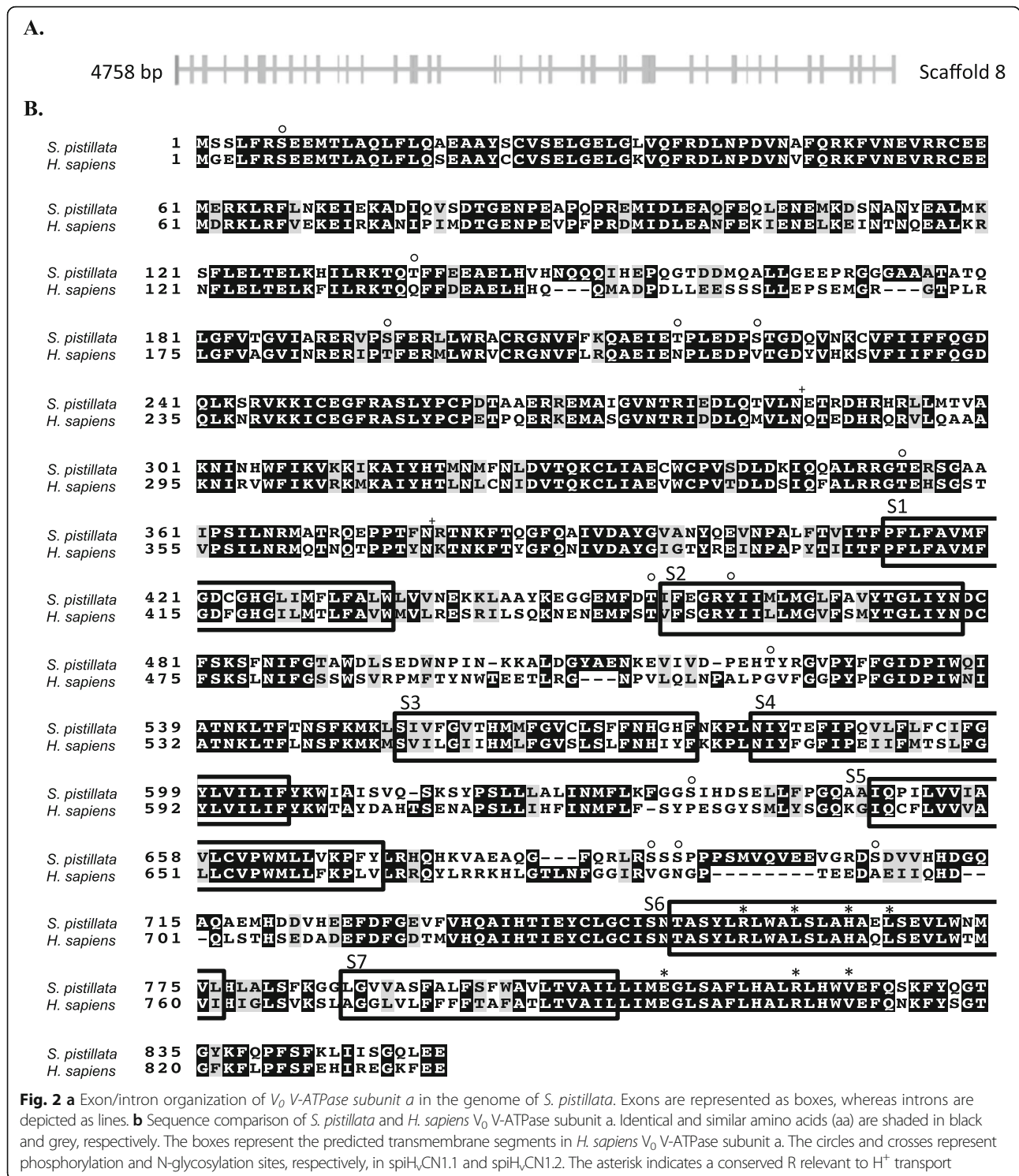
### Candidate voltage-gated $H^+$ channels ( $H_vCN$ ) in *S. pistillata*: gene structures, amino acid sequences and phylogenetic analysis

Data mining in the genome and transcriptome of *S. pistillata* allowed us to identify two genes, *spiH<sub>v</sub>CN1.1* and *spiH<sub>v</sub>CN1.2*, homologous to human *hH<sub>v</sub>CN1*. The gene and transcript information of the two *spiH<sub>v</sub>CN* genes is given in Fig. 4a and Additional file 2.



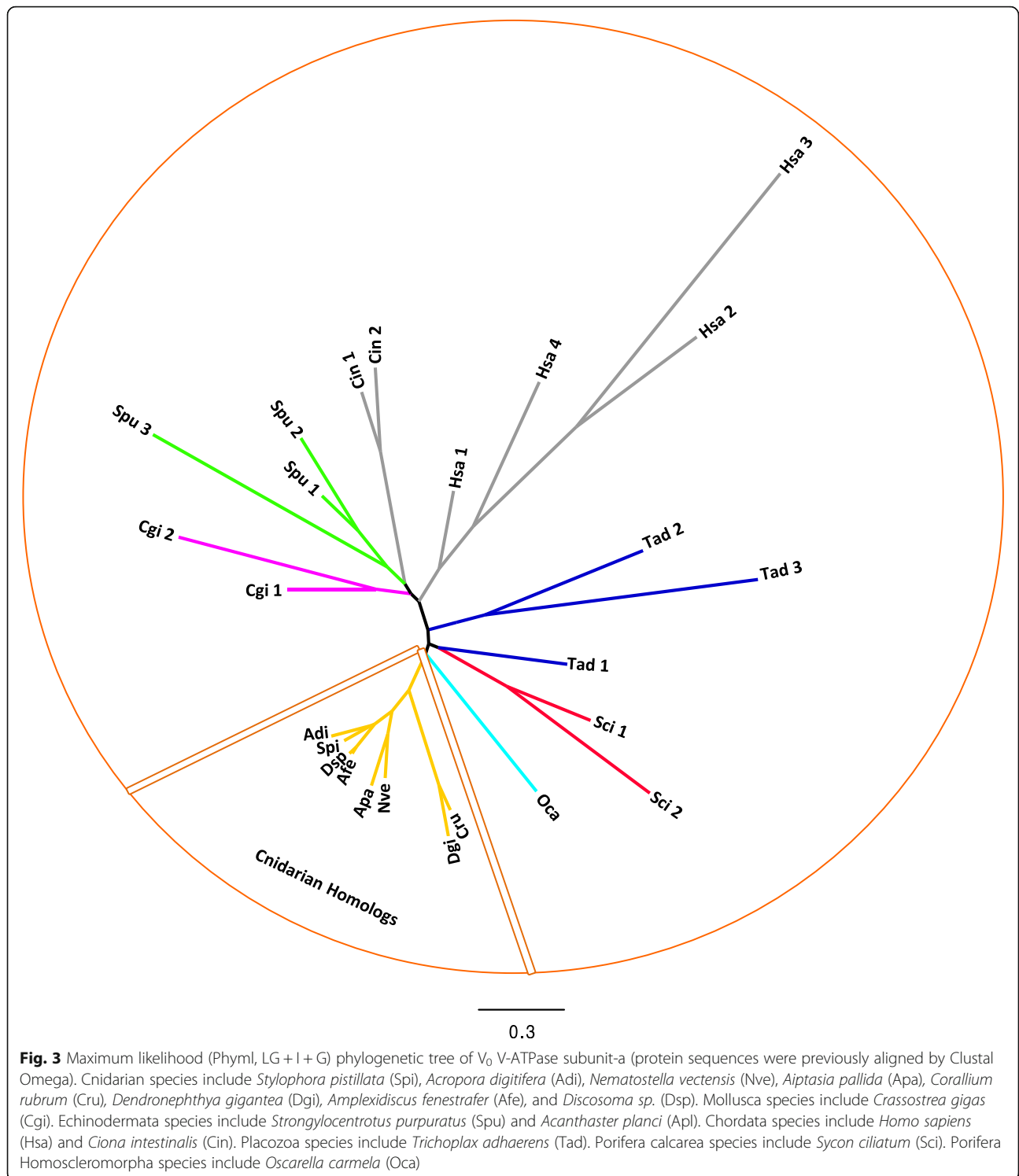
spiH<sub>v</sub>CN1.1 and spiH<sub>v</sub>CN1.2 share 35% identity and 62% similarity and possess four predicted transmembrane domains (TMs) (Additional file 3). The TMs display sequence conservation (Fig. 4b), with highly

conserved residues relevant to H<sub>v</sub>CN activity mostly located in the TMs. The two spiH<sub>v</sub>CN sequences exhibit similarity with hH<sub>v</sub>CN1: spiH<sub>v</sub>CN1.1 has 40% identity and 67% similarity to hH<sub>v</sub>CN1, and



spiH<sub>v</sub>CN1.2 has 28% identity and 61% similarity to hH<sub>v</sub>CN1. Several basic and acidic residues (R205, R208, R211, H140, E153 and D174) are conserved between spiH<sub>v</sub>CNs and hH<sub>v</sub>CN1, whereas the residues D112, D123, D185 and E119 are conserved only

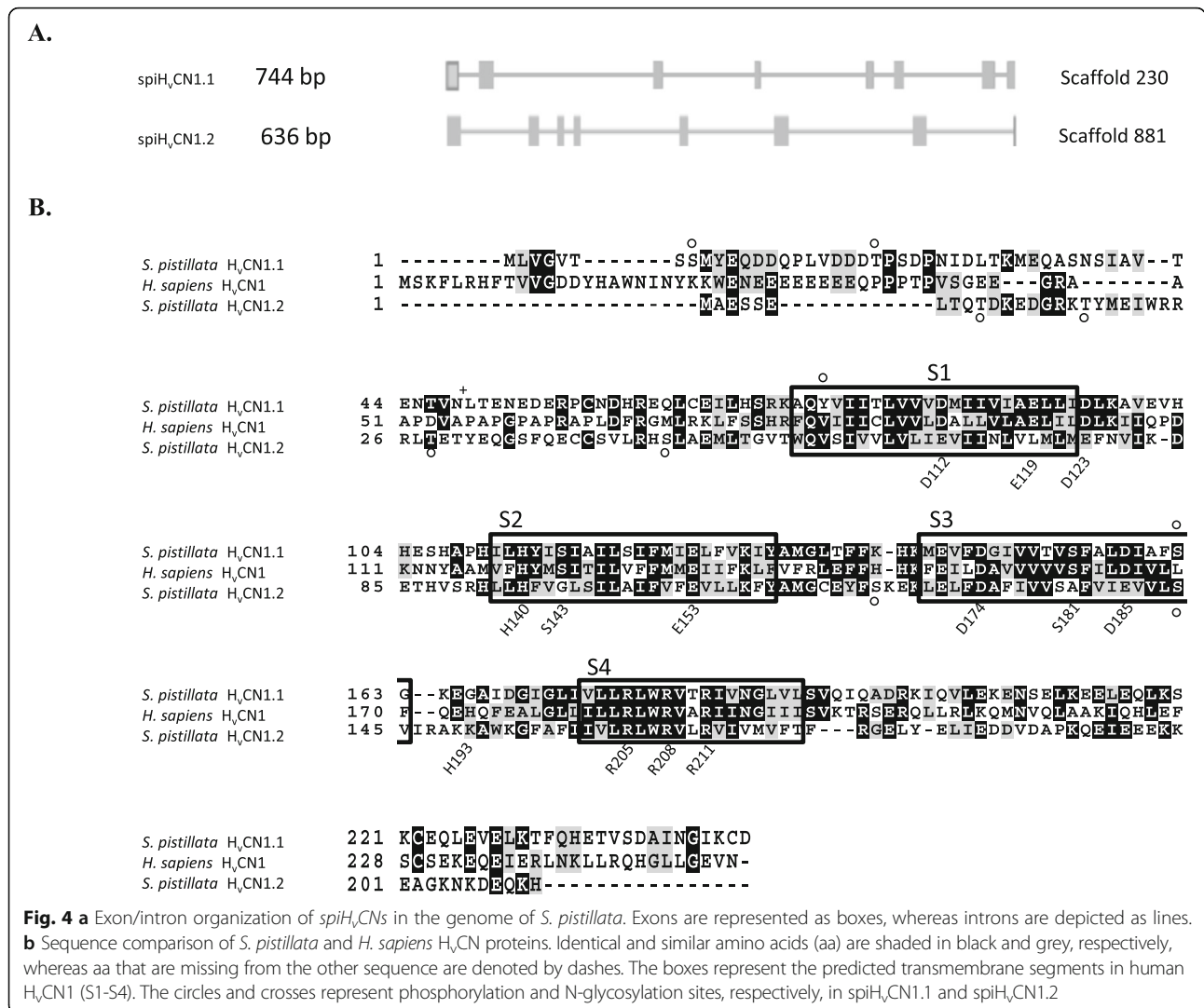
between spiH<sub>v</sub>CN1.1 and hH<sub>v</sub>CN1. Regarding post-translational modifications, several phosphorylation sites were predicted for both spiH<sub>v</sub>CNs, whereas N-glycosylation sites were predicted only for spiH<sub>v</sub>CN1.1 (Additional file 7).



Sequence similarity searches of available proteomic and genomic datasets using the human  $H_VCN1$  protein identified putative  $H_VCN$  homologs in several evolutionarily distant species (Fig. 5). Members of Hexacorallia are the only species that possess two  $H_VCN$ s, which splits the tree into two groups:  $H_VCN1.1$  and  $H_VCN1.2$ .

### Tissue-specific gene expression of *S. pistillata* $H^+$ transporters

Quantitative real-time PCR was used to detect  $H^+$  transporter mRNA expression (relative mRNA quantification,  $R_q$ ) in the oral fraction and the total colony (prepared according to Ganot et al., 2015 and Zoccola et al., 2015)



of *S. pistillata*. The results showed no differential expression of *spiSLC9A1*, *spiSLC9B1*, *spiSLC9B2* or *spiV<sub>0</sub> V-ATPase subunit-a* (Fig. 6a, e, f and g and Additional file 9) between the two coral fractions. *spiSLC9A6* and *spiSLC9A7* (Fig. 6b and c) were more highly expressed ( $p$ -value = 0.023 and 0.018, respectively) in the oral fraction than in the total colony, and *spiSLC9A8* (Fig. 6d) was more highly expressed ( $p$ -value = 0.108) in the total colony than in the oral fraction. Finally, *spiH<sub>v</sub>CN1.1* (Fig. 6h) was more highly expressed ( $p$ -value = 0.107) in the total colony than in the oral fraction, whereas *spiH<sub>v</sub>CN1.2* (Fig. 6i) was more highly expressed ( $p$ -value = 0.007) in the oral fraction than in the total colony.

**Effect of ocean acidification on the gene expression of *S. pistillata* H<sup>+</sup> transporters**

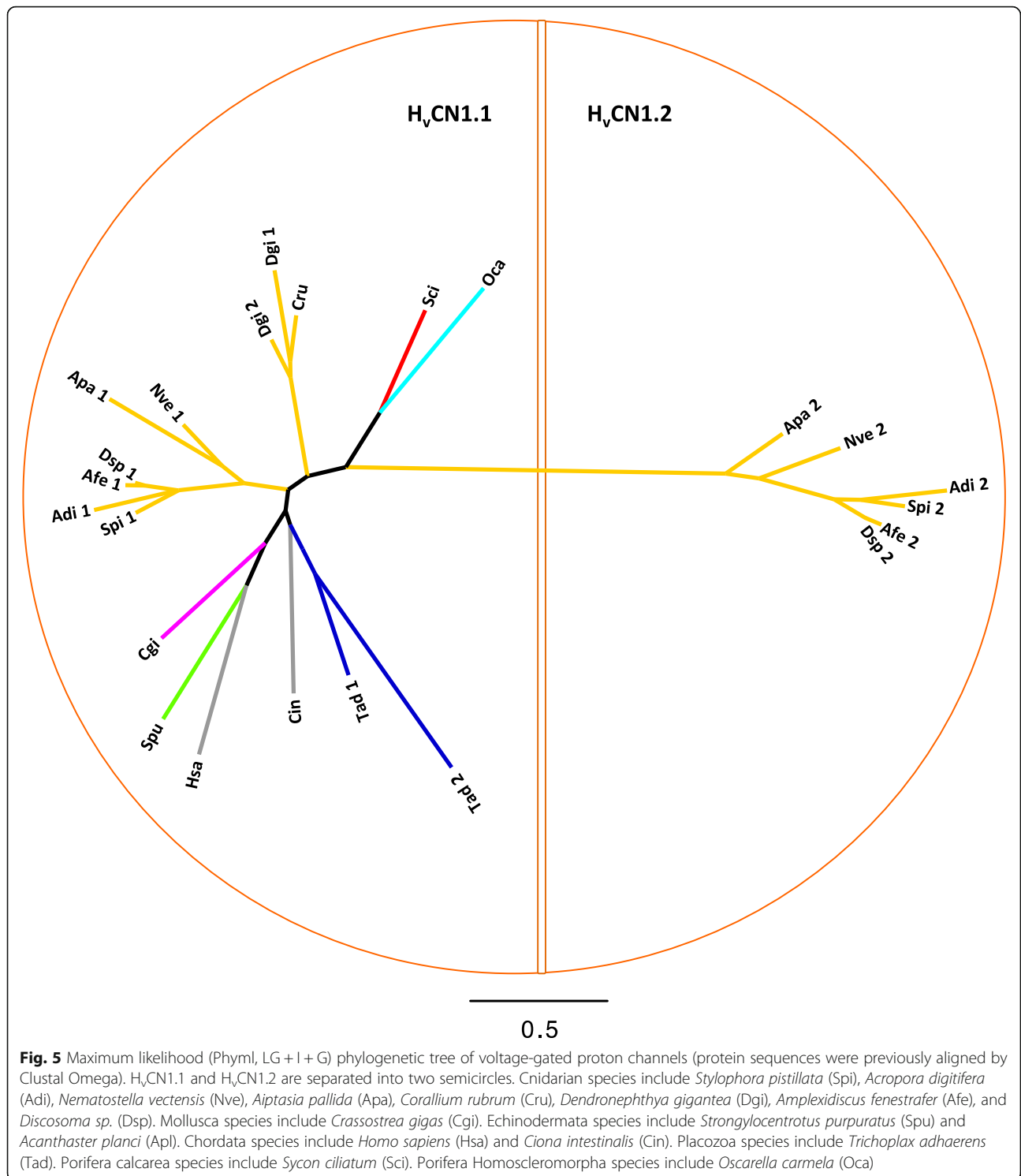
To study the effect of seawater acidification on H<sup>+</sup> transporter mRNA expression, real-time qPCR analysis of the

*spiSLC9A-B*, *spiV<sub>0</sub> V-ATPase subunit-a* and *spiH<sub>v</sub>CN* genes was carried out in *S. pistillata* micro-colonies exposed to control and acidified seawater (pH 8.1 and 7.2, respectively) for two different durations: 1 week and 1 year. The results showed that there was no difference in the expression of these genes between micro-colonies exposed to pH 8.1 and pH 7.2 for 1 week (Fig. 7 and Additional file 10). After 1 year of exposure to lower pH, there was no difference in the expression of most H<sup>+</sup> transporter-coding genes (Fig. 8 and Additional file 10). Only *spiSLC9A1* was more highly expressed ( $p$ -value = 0.029) at pH 7.2 than at the control pH of 8.1 (Additional file 10).

**Discussion**

**Phylogeny, domain topology and motif analysis of SLC9s from *S. pistillata***

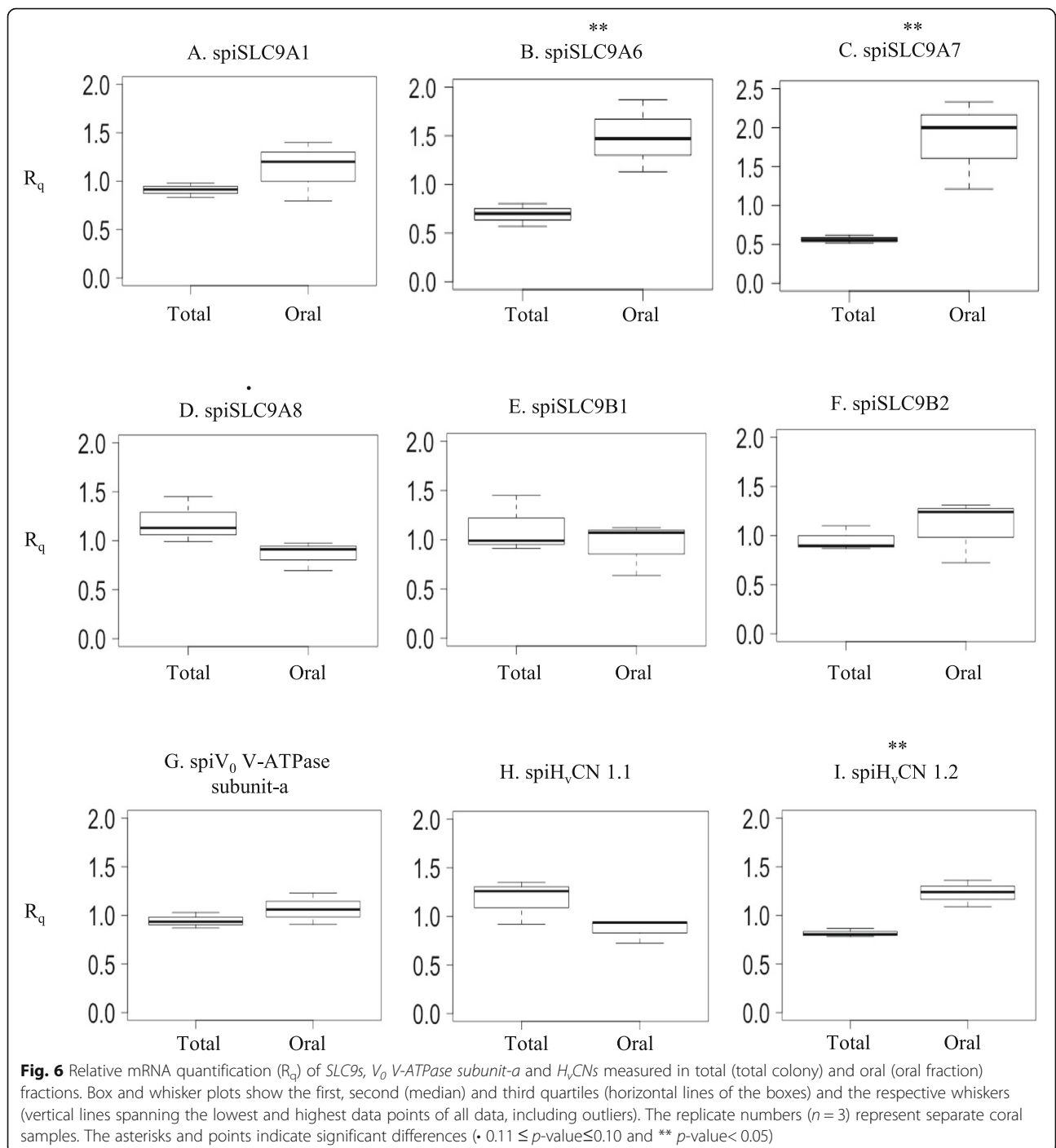
We identified SLC9 homologs in all anthozoan species (Fig. 1). The anthozoan SLC9 proteins cluster within at



least one subfamily (A, B and C), as previously described, suggesting a common ancestor at the time of Bilateria-Radiata separation.

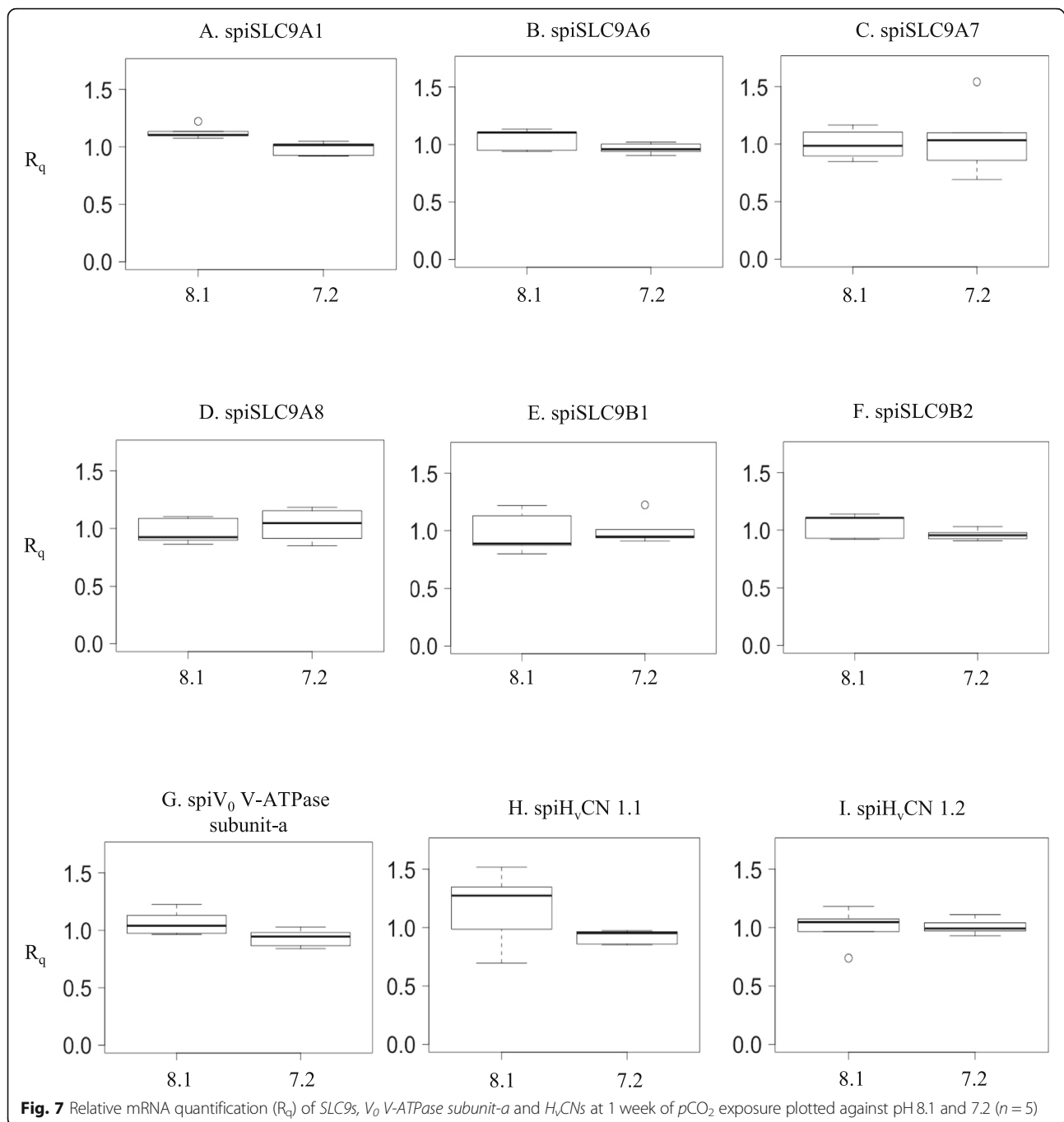
The spiSLC9s characterized in *S. pistillata* show similar characteristics to those of human SLC9s [25, 48], such as a highly homologous transmembrane domain

and a variable cytosolic domain. In addition, several key residues important for the function of hSLC9s are also conserved in spiSLC9s. For the A subfamily (Additional file 4), these residues include F161, which is important for Na<sup>+</sup> transport and acts as a pore-lining residue [49]; P167 and P168, which play a structural role in the



folding of the transmembrane domain [50] and influence the targeting and expression of SLC9A proteins [49]; and R440 and G455/G456, which are located in the so-called “glycine rich region” and contribute to the proper functioning of the putative “pH<sub>i</sub> sensor” domain [51]. For the B subfamily (Additional file 5), the conserved features between the human and *S. pistillata* homologs are especially apparent between glycine zipper (GZ) sequences. GZ sequences mediate close helix-helix folding

within transmembrane structures and facilitate the formation of membrane pores. This feature might facilitate access to the mitochondrial inner membrane, where these proteins are highly abundant [52]. Finally, the members of subfamily C (Additional file 6) contain two domains that are conserved with the human homolog: the VSD and the CNBD. The VSD of spiSLC9C carries positively charged residues (K and R) in S4 that are also strongly conserved in the SLC9C of *Strongylocentrotus*



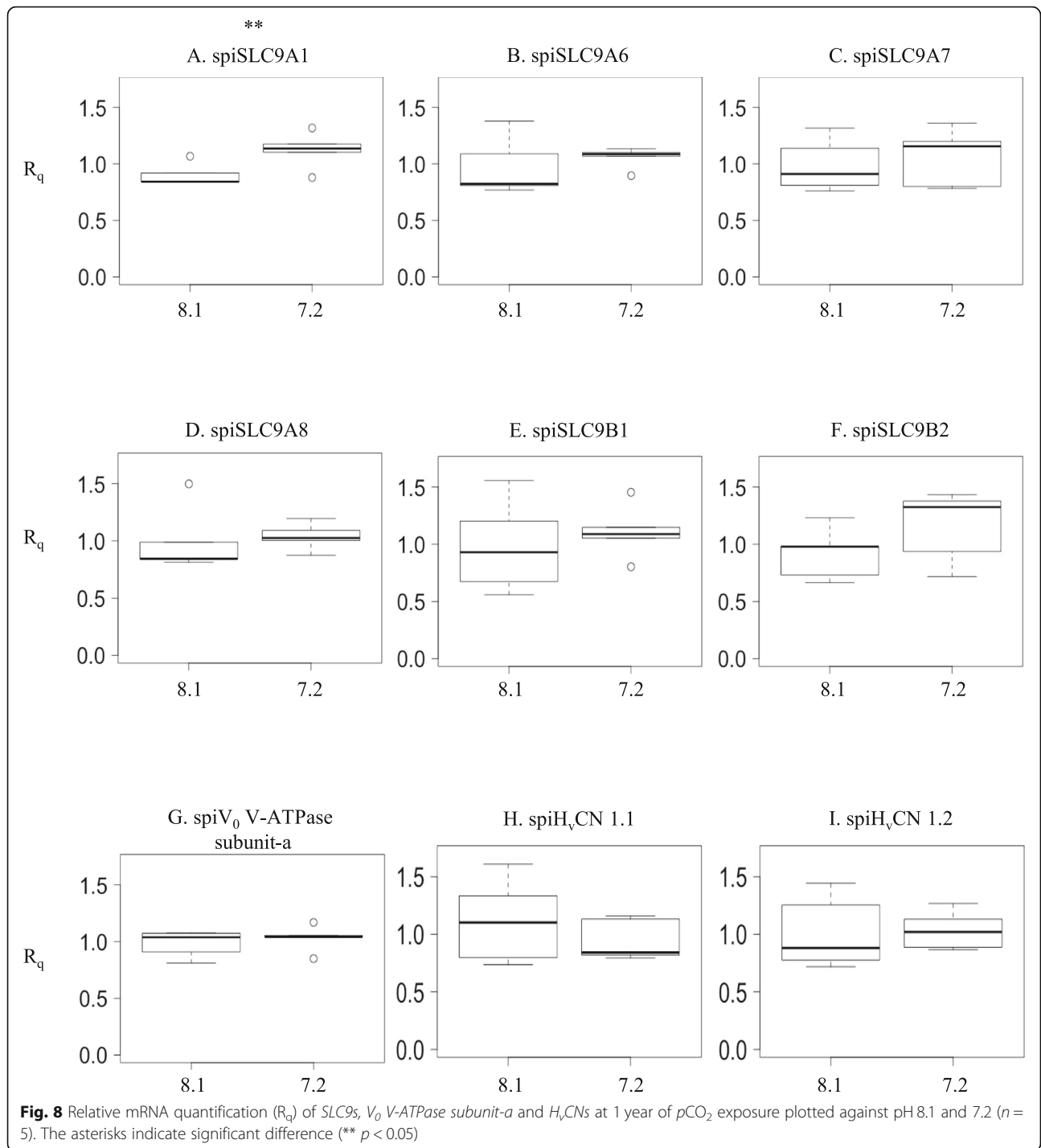
*purpuratus*, *Ciona intestinalis*, *Lepisosteus oculatus* and *Drosophila melanogaster* [53]. Some of these residues are missing in *Homo sapiens*, suggesting that voltage activation differs between these species and humans. The CNBD also regulates the activity of spiSLC9C, probably through the binding of cyclic adenosine monophosphate (cAMP) produced by the soluble adenylyl cyclase enzyme (sAC), as reported in the sea urchin [53].

Overall, the conserved features of spiSLC9s align with their roles as  $\text{Na}^+/\text{H}^+$  exchangers. Their shared

properties with previously characterized SLC9s indicate that they retain similar functions and provide insights into their activation mechanism and regulation in *S. pistillata*.

#### Phylogeny, domain topology and motif analysis of *V<sub>0</sub> V-ATPase subunit-a* from *S. pistillata*

We identified *V<sub>0</sub> V-ATPase subunit-a* homologs in Anthozoa (Fig. 3). In contrast to most species, which possess more than one *V<sub>0</sub> V-ATPase subunit-a* homolog,



anthozoans possess only one. This suggests that the specialization of  $V_0$  V-ATPase subunit-a homologs could be phylum-specific or even species-specific [54].

$V_0$  V-ATPase subunit-a in *S. pistillata* shares similar characteristics with those in yeast and humans, including the number of predicted TMs, which falls within the TM range of its homologs (5–8 TMs) [55]. TMs are thought to form proton-conducting hemichannels that

allow  $H^+$  to translocate across the membrane [56]. Previous studies in yeast allowed the identification of functional residues in  $V_0$  V-ATPase subunit-a through the use of random and site-direct mutagenesis. Among these residues, R735 is known to play an essential role in proton transport, as mutations of this residue result in complete inactivation of the ATP-dependent  $H^+$  transport of the V-ATPase [26]. The conservation of this

residue in *S. pistillata* suggests that R735 fulfils its role in H<sup>+</sup> transport (Fig. 2b). Other residues (L739, H743, L746, E789, R799 and V803) involved in proton translocation and ATPase activity [55] are also conserved in *S. pistillata*.

Overall, the features conserved between spiV<sub>0</sub> V-ATPase subunit-a and its human and yeast homologs align with its role as the subunit-a of the V<sub>0</sub> V-ATPase. Furthermore, the identification of homologs of all the V-ATPase subunit-encoding genes in the genome and transcriptome of *S. pistillata* (Additional file 8) suggests a conserved organization between the *S. pistillata* V-ATPase and the human V-ATPase.

### Phylogeny, domain topology and motif analysis of H<sub>v</sub>CNs from *S. pistillata*

One H<sub>v</sub>CN family member (H<sub>v</sub>CN1.1) was identified in all species examined in this study, including the four anthozoan orders, namely, Actinaria, Alcyonacea, Corallimorpharia and Scleractinia (Fig. 5). In addition, we report for the first time a second member of the H<sub>v</sub>CN family (H<sub>v</sub>CN1.2) in some Cnidaria. Genomic and transcriptomic searches of H<sub>v</sub>CN1.2 in public databases of Octocorallia and Hydrozoa (*Hydra magnipapillata*) did not produce any results (data not shown). The selective expression of H<sub>v</sub>CN1.2 only in Hexacorallia suggests that it is specific to this cnidarian subclass, and its presence in noncalcifying anthozoans (Corallimorphs and Actinaria) suggests that it is not linked to the appearance of aragonite biomineralization in Scleractinia [57]. The two voltage-gated proton channels (spiH<sub>v</sub>CNs) characterized in *S. pistillata* are highly divergent. This finding is further supported by the length of the phylogenetic branch (Fig. 5) that separates the two homologs: the amino acid similarity between spiH<sub>v</sub>CN1.1 and hH<sub>v</sub>CN1.1 is higher than that between spiH<sub>v</sub>CN1.1 and spiH<sub>v</sub>CN1.2.

The spiH<sub>v</sub>CNs possess molecular properties that are hallmarks of all H<sub>v</sub>CNs, such as the four transmembrane segments, the basic (R) and acidic residues (D and E) associated with voltage sensing, and the coiled-coil structure at the C-terminus [58]. The gating of proton channels is tightly regulated by pH and voltage, ensuring that they open only to extrude H<sup>+</sup> from the cell [43]. Phosphorylation of the spiH<sub>v</sub>CNs might activate these channels and enable them to open faster and at less positive voltages than those required without activation, as previously reported in human leukocytes [59–62].

SpiH<sub>v</sub>CN1.1 and spiH<sub>v</sub>CN1.2 share similar structures and organizations (Fig. 4). However, differences identified at the protein sequence level might reflect some unique features. First, many acidic residues, which are known to be associated with voltage sensing in hH<sub>v</sub>CN1 [58, 63], are present in spiH<sub>v</sub>CN1.1 but not in

spiH<sub>v</sub>CN1.2. This could result in a different sensitivity to voltage, with spiH<sub>v</sub>CN1.2 being less sensitive than spiH<sub>v</sub>CN1.1. Additionally, among these residues, D112 in S3, which is known to be essential for proton and charge selectivity [61], is missing and replaced by E112 in spiH<sub>v</sub>CN1.2. However, a previous study demonstrated that the substitution of D112 with an acidic residue in the same position maintained proton specificity in hH<sub>v</sub>CN1 [61], suggesting that both spiH<sub>v</sub>CNs are proton specific. Another difference concerns the Zn<sup>+2</sup>-binding residues of spiH<sub>v</sub>CNs. In humans and mice, proton currents are suppressed by extracellular Zn<sup>+2</sup>, which binds to four Zn<sup>+2</sup>-coordinating residues (E119, D123, H140 and H193) [64, 65]. By sequence comparison, we observed that at these positions, some residues are not conserved in spiH<sub>v</sub>CN1.1 (H193G) and are even less conserved in spiH<sub>v</sub>CN1.2 (E119L, D123E and H193K). Hence, we suggest that the replacement of Zn<sup>+2</sup>-coordinating residues with other residues potentially affects the Zn<sup>+2</sup> sensitivity of spiH<sub>v</sub>CNs, as reported in vertebrates [66, 67]. Since spiH<sub>v</sub>CN1.1 contains more Zn<sup>+2</sup>-coordinating residues, we propose that it is more sensitive to Zn<sup>+2</sup> than spiH<sub>v</sub>CN1.2.

Overall, the conserved features of the spiH<sub>v</sub>CNs align with their roles as voltage gated H<sup>+</sup>-channels. Common properties between the spiH<sub>v</sub>CNs and hH<sub>v</sub>CN preserve their voltage sensitivity and proton specificity, with some differences concerning their Zn<sup>+2</sup> sensitivity. In addition, distinctive properties between different spiH<sub>v</sub>CNs suggest differential regulation, possibly linked to their localization/function. Future analyses, however, are required to validate these assumptions and provide insight into their physiological role.

### Tissue-specific expression patterns of H<sup>+</sup> transporter genes in *S. pistillata*

Whole coral colonies are typically used in conventional techniques of gene expression analysis, limiting the possibility of further differentiating specific gene expression between oral and aboral tissues. These tissues contain different cell subtypes; some of them are more abundant (e.g., endosymbiotic dinoflagellates) or exclusively found (e.g., cells specialized for food digestion and reproduction, nematocysts) in the oral tissue, whereas others are exclusively found in the aboral tissue (e.g., calcifying cells) (Veron et al., 1993; Peter et al., 1997) [68]. As several physiological functions are associated with these cellular subtypes, analysing the differential gene expression of H<sup>+</sup> transporters in the two coral tissues helps identify the potential physiological processes in which they might participate.

To perform this task, we used a previously developed micro-dissection protocol [20, 69] to separate the oral fraction (including the oral disc and most of the polyp

body, with no or minimal contamination of cells from the aboral tissue) from the total colony. We then compared the expression of H<sup>+</sup> transporters in the oral fraction to that in the total colony.

Our results demonstrate that some H<sup>+</sup> transporters are more highly expressed in the oral fraction than in the total colony (hereafter referred to as “oral-specific”); others are more highly expressed in the total colony than in the oral fraction (hereafter referred to as “aboral-specific”); and others are expressed at the same levels in both fractions (hereafter referred to as “ubiquitous”) (Fig. 6). Using H<sup>+</sup> transporter tissue expression and the existing literature in other systems as supporting information, we discuss the role that these transporters might play in corals.

The oral-specific H<sup>+</sup> transporters include spiSLC9A6, spiSLC9A7 and spiH<sub>v</sub>CN1.2. spiSLC9A6 and spiSLC9A7 are organellar homologs (Fig. 1), and as reported for humans [48, 70], they might play a role in vesicular neurotransmitter uptake in oral polyps, where an elaborate nerve ring system is present [71]. In addition, cells in the oral tissue are enriched with zooxanthellae [72], which produce and incorporate high levels of anionic superoxide (e.g., throughout photosynthesis) and Zn<sup>+2</sup> (e.g., through uptake from seawater) that accumulate in the host cytoplasm [73–75]. Thus, spiH<sub>v</sub>CN1.2 might favour the exit of H<sup>+</sup> at the basolateral membrane of these cells, as reported in human osteoblasts [76], preventing the membrane depolarization to extreme negative voltages associated with O<sub>2</sub><sup>-</sup> electron transfer. Additionally, the decreased Zn<sup>+2</sup> sensitivity of spiH<sub>v</sub>CN1.2 compared to that of spiH<sub>v</sub>CN1.1 (see Discussion 3.1.3) could be correlated with the higher Zn<sup>+2</sup> concentration levels in the oral (symbiotic) cells [67, 77–80].

The aboral-specific H<sup>+</sup> transporters are spiH<sub>v</sub>CN1.1 and spiSLC9A8. These transporters could play a role in the pH<sub>i</sub> regulation of calcifying cells. During the calcification reaction, H<sup>+</sup> is produced in the ECM and needs to be removed to promote an alkaline environment favourable for calcification [11, 81]. The Ca<sup>+2</sup>-ATPase at the apical side of the calcifying cells has been suggested to be involved in pumping out H<sup>+</sup> from the ECM [41]. On the basal side of the cell membrane, spiH<sub>v</sub>CN1.1 might contribute to extruding excess H<sup>+</sup> from the cytoplasm of calcifying cells, similar to the role it plays in coccolithophores [82]. Finally, the organellar spiSLC9A8 might regulate medial/trans-Golgi pH and intracellular trafficking, as in humans [83, 84], since in calcifying cells, this function is particularly necessary for the regulation of organic matrix synthesis and secretion [85].

The rest of the H<sup>+</sup> transporters (V<sub>0</sub> V-ATPase subunit-a, spiSLC9A1, spiSLC9B1 and spiSLC9B2) are ubiquitous. Our results suggest that the coral V<sub>0</sub> V-

ATPase subunit-a homolog is ubiquitously expressed and differs from those identified in humans. Indeed, the human V<sub>0</sub> V-ATPase subunit-a isoforms have different tissue distributions with intracellular or apical/basolateral membrane localization [31, 55, 86–89]. This difference is probably linked to the primers used for the detection of the coral V<sub>0</sub> V-ATPase subunit-a, which do not discern the different isoforms (X1, X2, X3 and X4; see Additional file 8) but recognize all of them. We suggest that other ubiquitous transporters play housekeeping roles. spiSLC9A1, for example, could play a role in homeostatic pH regulation on the basolateral cell membrane, and spiSLC9B1–2 might participate in organismal ion homeostasis on the mitochondrial inner membrane, as reported in vertebrates [19, 90–93]. Interestingly, spiSLC9A1 was the only transporter affected by seawater acidification after 1 year of exposure (Fig. 8). Its activation might be triggered by the pH<sub>i</sub> sensor domain (see Discussion 3.1.1), which activates the transporter at low pH<sub>i</sub> values, similar to humans [19]. Figure 9 summarizes the tissue distribution of the principal acid-base transporters that could participate in the intracellular pH regulation of coral cells based on the results obtained by performing real-time PCR of oral fraction and total colony coral samples. These transporters include the H<sup>+</sup> transporters SLC9, V-ATPase and H<sub>v</sub>CN, which were characterized in the present study, and the HCO<sub>3</sub><sup>-</sup> transporters SLC4 and SLC26, which were characterized by Zoccola et al. in 2015.

## Conclusions

This study provides the first molecular characterization in the coral *S. pistillata* of several families of H<sup>+</sup> transporters, which are known as pH<sub>i</sub> regulators in animal cells. Most importantly, we report for the first time a novel member of the H<sub>v</sub>CN gene family, H<sub>v</sub>CN1.2, in the cnidarian subclass Hexacorallia. The identification of conserved residues between coral and human H<sup>+</sup> transporter homologs suggests functional conservation related to intracellular pH<sub>i</sub> regulation.

However, additional experiments (e.g., gene silencing experiments, pharmacological experiments using inhibitors, electrophysiological measurements of H<sup>+</sup> currents, etc.) with a larger number of replicates need to be carried out in the future to demonstrate the participation of these H<sup>+</sup> transporters in coral acid-base cellular homeostasis. Moreover, we assessed the tissue specificity of the H<sup>+</sup> transporter gene families in the coral *S. pistillata*, and we observed that their expression was not restricted to only one specific tissue (oral or aboral), as reported for some members of the HCO<sub>3</sub><sup>-</sup> gene family [20]. However, we observed higher or lower expression profiles in the oral or aboral tissues. These results both highlight the importance of H<sup>+</sup> transporters in the coral colony



(See figure on previous page.)

**Fig. 9** Model of acid-base transporters involved in intracellular pH regulation expressed on the apical (AM) and basolateral (BLM) membranes of coral cells throughout the tissue layers. The roles of other ion channels and transporters involved in other cellular processes are not considered here. Transporters that are more highly expressed in the oral fraction (oral-specific) are coloured in blue, those that are more highly expressed in the total colony (aboral-specific) are coloured in orange, and those that are expressed at the same levels in both fractions (ubiquitous) are coloured in green. Other enzymes (CA = carbonic anhydrase) and transporters (PMCA =  $\text{Ca}^{+2}$  ATPase) involved in the  $\text{H}^+$  flux balance are represented in bold letters

and suggest that they take part in homeostatic (e.g., intracellular acid-base balance) and physiological processes (e.g., calcification, photosynthesis, food digestion). Finally, we investigated the impact of OA on  $\text{H}^+$  transporter gene expression in *S. pistillata*, and we identified one candidate gene (*spiSLC9A1*) involved in the coral response to ocean acidification that showed differential expression after long-term exposure to acidified seawater (1 year). The other  $\text{H}^+$  transporters did not show any significant changes at the gene level under seawater acidification conditions. Nevertheless, the modulation of gene expression can also occur at the protein level, which should be investigated in future studies. The influence of other environmental factors, e.g., temperature, remains to be tested and will enrich the understanding of coral phenotypic plasticity. This knowledge is especially relevant to our understanding of the ability of benthic animals to buffer the impacts of environmental changes, thereby providing more time for genetic adaptation to occur. In addition, responses to environmental changes are often species-specific [9], with physiological differences that can potentially reflect a different profile of  $\text{H}^+$  transporter gene expression, which could also be investigated in other coral species. Such comparative studies might aid in the development of molecular markers linked to  $\text{pH}_i$  tolerance traits in coral reef populations.

## Methods

### Biological materials

Experiments were conducted on the symbiotic scleractinian coral *Stylophora pistillata* grown in the long-term culture facilities at the Centre Scientifique de Monaco in aquaria supplied with seawater from the Mediterranean Sea (exchange rate  $2\% \text{ h}^{-1}$ ) under the following controlled conditions: semi-open circuit, temperature of  $25^\circ\text{C}$ , salinity of 38, light exposure of  $200 \mu\text{mol photons m}^{-2} \text{ s}^{-1}$ , and a 12 h:12 h light:dark cycle. Samples were prepared from one mother colony as nubbins suspended on monofilament threads. After 3 weeks of cicatrisation, the first set of samples ( $n = 3$ ) was used for the oral fraction micro-dissection experiment, and another set ( $n = 20$ ) was used for the exposure to seawater acidification experiment.

### Exposure to seawater acidification

The seawater acidification setup was performed as described previously [9, 94, 95]. Briefly, carbonate

chemistry was manipulated by bubbling with  $\text{CO}_2$  to reduce the pH from the control value of pH 8.1 to the target value of 7.2. Twenty coral nubbins were randomly distributed among four experimental tanks ( $n = 5$  for each experimental tank): two tanks (pH 8.1 and 7.2) were reserved for 1 week of exposure, and two were reserved for 1 year of exposure. The experiments were repeated three times to ensure reliability. Similar results were obtained for each experiment (not shown).

### Data mining

The amino acid sequences of human  $\text{H}^+$  transporters were retrieved from NCBI (<http://www.ncbi.nlm.nih.gov/protein>) and used as a bait to mine (BLAST) the transcriptome, genome and EST databases of the following phyla: Cnidaria (*Stylophora pistillata*, *Acropora digitifera*, *Nematostella vectensis*, *Aiptasia pallida*, *Amplexidiscus fenestrafer*, *Discosoma sp.*, *Corallium rubrum* and *Dendronephthya gigantea*), Mollusca (*Crassostrea gigas*), Echinodermata (*Strongylocentrotus purpuratus*), Chordata (*Ciona intestinalis*), Porifera (*Sycon ciliatum*) and Placozoa (*Trichoplax adhaerens*). The following web servers were used: NCBI (<http://www.ncbi.nlm.nih.gov/>), EnsemblMetazoa (<https://metazoa.ensembl.org/>), ReefGenomics (<http://reefgenomics.org>) and Cnidarian Database (<http://data.centrescientifique.mc/>).

### Sequence analysis

Putative transmembrane helices in proteins were predicted by the Center for Biological Sequence Analysis Prediction Server (<http://www.cbs.dtu.dk/services/>) using the TMHMM algorithm. On the same platform, phosphorylation and N-glycosylation prediction analyses were performed using NetPhos and NetNGlyc.

### Phylogenetic analyses

Alignment of  $\text{H}^+$  transporter amino acid sequences was performed using Clustal Omega on the EMBL-EBI server (<https://www.ebi.ac.uk/>). Based upon the produced amino acid alignments, maximum likelihood estimates of the topology and the branch length were obtained using PhyML v3.1 [96]. The model of substitution used in this step was LG + G, which was previously selected over others via alignment analysis with ProtTest3.4.2 [97]. Phylogenetic trees were then edited using FigTree v1.4.4 (Rambaut et al., 2014).

### Oral fraction micro-dissection

Coral micro-dissection was performed as indicated previously [20, 69]. Briefly, coral nubbins ( $n = 3$ ) were set to rest in a glass petri dish filled with seawater and tricaine mesylate. Once polyps were extended, oral fractions (including the oral disc and most of the polyp body) were cut from the coral colony (total colony) using micro-dissection scissors under a binocular microscope. Both fractions (oral fraction and total colony) were then used for RNA extraction.

### Real-time PCR (qPCR)

Total RNA extraction and cDNA synthesis were performed as described previously [98]. Briefly, RNA was isolated from biological triplicates that underwent micro-dissection or from quintuplicates collected for each pH treatment using an RNeasy kit (Qiagen) according to the manufacturer's instructions. Reverse transcription was then performed using SuperScript IV Reverse Transcriptase (Invitrogen) on 2  $\mu\text{g}$  of RNA. Thermo cycler conditions were set as follows: 50 min at 50 °C, 7 min at 25 °C, 50 min at 50 °C and 5 min at 85 °C. qPCR runs were performed in 96-well plates on a QuantStudio 3 (Applied Biosystems) machine using PowerUp™ SYBR™ Green Master Mix for PCR amplification. The primer sequences used are provided in Additional file 11. Relative expression was calculated using Biogazelle qBase + 2.6TM [99]. Gene expression was normalized (relative mRNA quantification, Rq) to the expression of two reference genes, ubiquitin-60S ribosomal protein (L40) [100] and an acidic ribosomal phosphoprotein P0 (36B4) [101], after these genes were determined to have acceptably low M values and coefficients of variation [99].

### Statistical analysis

Statistical analysis was performed using R v3.5.2 software. For the oral fraction micro-dissection experiment, a fixed number of samples ( $n = 3$ ) was used due to technical limitations. For the exposure to seawater acidification experiment, a sample size estimation was performed, and  $n = 5$  samples were used. For both experiments, the normal distribution of the data was evaluated using Shapiro-Wilk's test. Samples with a standard deviation  $\geq 5$  were excluded from the analysis. This was the case for *spiSLC9C*, whose qPCR results showed great variability, probably due to its extremely low expression values. A t-test was used to identify differentially expressed genes between *S. pistillata* fractions (oral fraction and total colony) and pH treatments (pH 8.1 and pH 7.2). We considered  $0.10 \leq p$ -values  $\leq 0.11$  to indicate near-marginal significance ( $\bullet$ );  $p$ -values  $\leq 0.1$  as significant (\*\*); and  $p$ -values  $\leq 0.05$  as highly significant (\*).

### Abbreviations

CNBD: Cyclic nucleotide-binding domain; CPA1: Cation proton antiporter 1; CPA2: Cation proton antiporter 2; ECM: Extracellular calcifying medium; GZ: Glycine zipper;  $H_vCN$ : Voltage-gated proton channel; NaT-DC: Na-transporting carboxylic acid decarboxylase; OA: Ocean acidification; sAC: Soluble adenylyl cyclase; SLC9: Solute carrier 9; TM: Transmembrane segment; V-ATPase: Vacuolar-type electrogenic  $H^+$ -ATP hydrolase; VSD: Voltage-sensing domain

### Supplementary Information

The online version contains supplementary material available at <https://doi.org/10.1186/s12860-021-00353-x>.

**Additional file 1.** Exon/intron organization of *SLC9s* in the genome of *S. pistillata*.

**Additional file 2.** Gene and transcript information of  $H^+$  transporter family members in *S. pistillata*.

**Additional file 3.** Transmembrane segment prediction (TMs) of  $H^+$  transporter proteins in *S. pistillata*.

**Additional file 4.** Sequence comparison of the *H. sapiens* SLC9A1 and *S. pistillata* SLC9A proteins.

**Additional file 5.** Sequence comparison of the *S. pistillata* and *H. sapiens* SLC9B proteins.

**Additional file 6.** Sequence comparison of the *S. pistillata* and *H. sapiens* SLC9C1 proteins. The boxes represent human voltage-sensing domains (S1-S4), and the asterisks indicate conserved positively and negatively charged residues relevant to voltage sensing. The rectangles indicate conserved positively charged residues in S4 that are present in *S. pistillata* but missing in hSLC9C1. The triangles indicate residues involved in the cyclic nucleotide-binding domain.

**Additional file 7.** Number of phosphorylation sites and N-glycosylation sites predicted for *S. pistillata*  $H^+$  transporters.

**Additional file 8.** A.  $V_0$  V-ATPase subunit-a isoforms in coral *S. pistillata*. B. Human and coral homologs of V-ATPase subunits.

**Additional file 9.** Statistical analysis of the relative mRNA quantification ( $R_q$ ) of *SLC9s*, *V\_0* V-ATPase subunit-a and *H\_vCNs* ( $N = 3$ ) in *S. pistillata* total (total colony) and oral (oral fraction) fractions.

**Additional file 10.** Statistical analysis of the relative mRNA quantification ( $R_q$ ) of *SLC9s*, *V\_0* V-ATPase subunit-a and *H\_vCNs* ( $n = 5$ ) at pH 8.1 and 7.2 after 1 week and 1 year of  $p\text{CO}_2$  exposure. The asterisks indicate significant differences (\*\*  $p < 0.05$ ).

**Additional file 11.** List of *S. pistillata*  $H^+$  transporter genes with RT-PCR primers and product sizes.

### Acknowledgements

We would like to thank Dominique Desgré for coral maintenance and Alexander Venn for kindly revising the text of the manuscript. This study was conducted as part of the Centre Scientifique de Monaco Research Program, which is supported by the Government of the Principality of Monaco.

### Authors' contributions

ST and DZ designed and conceived the study. LC conducted the study. LC, PG, VPB and DZ analysed the data. LC, ST and DZ wrote the manuscript. All authors read and approved the manuscript.

### Funding

Funding of this study was provided by the Government of the Principality of Monaco. The funding body played no role in the design, collection, analysis, or interpretation of the data; the writing of the manuscript; or the decision to submit the manuscript for publication.

### Availability of data and materials

All data needed to evaluate the conclusions in the paper are present in the manuscript and/or the Additional Files. Additional data related to this manuscript are available from the corresponding author on reasonable request. Genomic and transcriptomic data were obtained from the publicly

available database of the National Center for Biotechnology Information (<https://www.ncbi.nlm.nih.gov/>) or from the private database of the Centre Scientifique de Monaco (<http://data.centrescientifique.mc/>).

## Declarations

### Ethics approval and consent to participate

Not applicable.

### Consent for publication

Not applicable.

### Competing interests

The authors declare that they have no competing interests.

### Author details

<sup>1</sup>Centre Scientifique de Monaco, 8 quai Antoine 1er, 98000 Monaco, Monaco.

<sup>2</sup>Sorbonne Université, Collège Doctoral, F-75005 Paris, France.

Received: 16 October 2020 Accepted: 22 February 2021

Published online: 08 March 2021

## References

- Mumby PJ, Steneck RS. Coral reef management and conservation in light of rapidly evolving ecological paradigms. *Trends Ecol Evol*. 2008;23:555–63.
- Davies PS. Effect of daylight variations on the energy budgets of shallow-water corals. *Mar Biol*. 1991;108:137–44.
- Davy SK, Allemand D, Weis VM. Cell biology of cnidarian-Dinoflagellate Symbiosis. *Microbiol Mol Biol Rev*. 2012;76:229–61.
- Tambutté S, Tambutté E, Zoccola D, Allemand D. Organic Matrix and Biomineralization of Scleractinian Corals. In *Handbook of Biomineralization: Biological Aspects and Structure Formation* (pp.243 - 259), E. Bauerlein (Ed.). Kleyvas JA, Buddemeier RW, Archer D, Gattuso JP, Langdon C, Opdyke BN. Geochemical consequences of increased atmospheric carbon dioxide on coral reefs. *Science*. 1999;284(5411):118–20.
- Chan NCS, Connolly SR. Sensitivity of coral calcification to ocean acidification: a meta-analysis. *Glob Chang Biol*. 2013;19:282–90.
- Schoepf V, Grottoli AG, Warner ME, Cai WJ, Melman TF, Hoedley KD, et al. Coral energy reserves and calcification in a high-CO<sub>2</sub> world at two temperatures. *PLoS One*. 2013;8(10):e75049.
- Comeau S, Cornwall CE, McCulloch MT. Decoupling between the response of coral calcifying fluid pH and calcification to ocean acidification. *Sci Rep*. 2017;7:1–10. <https://doi.org/10.1038/s41598-017-08003-z>.
- Venn AA, Tambutté E, Caminiti-Segonds N, Techer N, Allemand D, Tambutté S. Effects of light and darkness on pH regulation in three coral species exposed to seawater acidification. *Sci Rep*. 2019;9:1–12.
- Tresguerres M, Hamilton TJ. Acid-base physiology, neurobiology and behaviour in relation to CO<sub>2</sub>-induced ocean acidification. *J Exp Biol*. 2017; 220:2136–48.
- Allemand D, Ferrier-Pagès C, Furla P, Houlbrèque F, Puverel S, Reynaud S, et al. Biomineralisation in reef-building corals: from molecular mechanisms to environmental control. *Comptes Rendus - Palevol*. 2004;3:453–67.
- Webb DJ, Nuccitelli R. Fertilization potential and electrical properties of the *Xenopus laevis* egg. *Dev Biol*. 1985;107:395–406.
- Venn AA, Tambutté E, Lottio S, Zoccola D, Allemand D, Tambutté S. Imaging intracellular pH in a reef coral and symbiotic anemone. *Proc Natl Acad Sci U S A*. 2009;106:16574–9.
- Laurent J, Tambutté S, Tambutté É, Allemand D, Venn A. The influence of photosynthesis on host intracellular pH in scleractinian corals. *J Exp Biol*. 2013;216:1398–404.
- Al-Horani FA, Al-Moghrabi SM, De Beer D. The mechanism of calcification and its relation to photosynthesis and respiration in the scleractinian coral *Galaxea fascicularis*. *Mar Biol*. 2003;142:419–26.
- Agostini S, Suzuki Y, Higuchi T, Casareto BE, Yoshinaga K, Nakano Y, et al. Biological and chemical characteristics of the coral gastric cavity. *Coral Reefs*. 2012;31:147–56.
- Cai WJ, Ma Y, Hopkinson BM, Grottoli AG, Warner ME, Ding Q, et al. Microelectrode characterization of coral daytime interior pH and carbonate chemistry. *Nat Commun*. 2016;7:1–8.
- Bove CB, Whitehead RF, Szmant AM. Responses of coral gastrovascular cavity pH during light and dark incubations to reduced seawater pH suggest species-specific responses to the effects of ocean acidification on calcification. *Coral Reefs*. 2020. <https://doi.org/10.1007/s00338-020-01995-7>.
- Casey JR, Grinstein S, Orłowski J. Sensors and regulators of intracellular pH. *Nat Rev Mol Cell Biol*. 2010;11:50–61. <https://doi.org/10.1038/nrm2820>.
- Zoccola D, Ganot P, Bertucci A, Caminiti-Segonds N, Techer N, Voolstra CR, et al. Bicarbonate transporters in corals point towards a key step in the evolution of cnidarian calcification. *Sci Rep*. 2015;5. <https://doi.org/10.1038/srep09983>.
- Barott KL, Barron ME, Tresguerres M. Identification of a molecular pH sensor in coral. *Proc R Soc B Biol Sci*. 2017;284.
- Tresguerres M, Barott KL, Barron ME, Deheyn DD, Kline DI, Linsmayer LB. Acid-Base Balance and Nitrogen Excretion in Invertebrates. *Acid-Base Balance Nitrogen Excretion Invertebr*. 2017:193–218.
- Nishigaki T, José O, González-Cota AL, Romero F, Treviño CL, Darszon A. Intracellular pH in sperm physiology. *Biochem Biophys Res Commun*. 2014; 450:1149–58. <https://doi.org/10.1016/j.bbrc.2014.05.100>.
- Orłowski J, Grinstein S. Diversity of the mammalian sodium/proton exchanger SLC9 gene family. *Pflugers Arch Eur J Physiol*. 2004;447:549–65.
- Donowitz M, Ming Tse C, Fuster D. SLC9/NHE gene family, a plasma membrane and organellar family of Na<sup>+</sup>/H<sup>+</sup> exchangers. *Mol Asp Med*. 2013;34:236–51.
- Kawasaki-Nishi S, Nishi T, Forgac M. Arg-735 of the 100-kDa subunit a of the yeast V-ATPase is essential for proton translocation. *Proc Natl Acad Sci U S A*. 2001;98:12397–402.
- Salvador JM, Inesi G, Rigaud JL, Mata AM. Ca<sup>2+</sup> transport by reconstituted synaptosomal ATPase is associated with H<sup>+</sup> countertransport and net charge displacement. *J Biol Chem*. 1998;273:18230–4.
- Brini M, Carafoli E. The plasma membrane Ca<sup>2+</sup> ATPase and the plasma membrane sodium exchanger cooperate in the regulation of cell calcium. *Cold Spring Harb Perspect Biol*. 2011 Feb 1;3(2):a004168.
- Perry SF, Beyers ML, Johnson DA. Cloning and molecular characterisation of the trout (*Oncorhynchus mykiss*) vacuolar H<sup>+</sup>-ATPase B subunit. *J Exp Biol*. 2000;203(Pt 3):459–70.
- Torigoe T, Izumi H, Ise T, Murakami T, Uramoto H, Ishiguchi H, et al. Vacuolar H<sup>+</sup>-ATPase: functional mechanisms and potential as a target for cancer chemotherapy. *Anti-Cancer Drugs*. 2002;13:237–43.
- Miranda KC, Karet FE, Brown D. An extended nomenclature for mammalian V-ATPase subunit genes and splice variants. *PLoS One*. 2010;5:1–5.
- Tresguerres M, Clifford AM, Harter TS, Roa JN, Thies AB, Yee DP, et al. Evolutionary links between intra- and extracellular acid–base regulation in fish and other aquatic animals. *J Exp Zool Part A Ecol Integr Physiol*. 2020; 333:449–65.
- DeCoursey TE. Voltage-gated proton channels. *Cell Mol Life Sci*. 2008;65: 2554–73.
- Lishko PV, Botchkina IL, Fedorenko A, Kirichok Y. Acid extrusion from human spermatozoa is mediated by flagellar voltage-gated Proton Channel. *Cell*. 2010;140:327–37.
- Stumpp M, Hu MY, Melzner F, Gutowska MA, Dorey N, Himmerkus N, et al. Acidified seawater impacts sea urchin larvae pH regulatory systems relevant for calcification. *Proc Natl Acad Sci U S A*. 2012;109:18192–7.
- Edwards SL, Claiborne JB, Morrison-Shetlar AI, Toop T. Expression of Na<sup>+</sup>/H<sup>+</sup> exchanger mRNA in the gills of the Atlantic hagfish (*Myxine glutinosa*) in response to metabolic acidosis. *Comp Biochem Physiol - A Mol Integr Physiol*. 2001;130:81–91.
- Claiborne JB, Edwards SL, Morrison-Shetlar AI. Acid-base regulation in fishes: cellular and molecular mechanisms. *J Exp Zool*. 2002;293:302–19.
- Li H, Ren C, Jiang X, Cheng C, Ruan Y, Zhang X, et al. Na<sup>+</sup>/H<sup>+</sup> exchanger (NHE) in Pacific white shrimp (*Litopenaeus vannamei*): molecular cloning, transcriptional response to acidity stress, and physiological roles in pH homeostasis. *PLoS One*. 2019;14:1–15. <https://doi.org/10.1371/journal.pone.0212887>.
- Hu MY, Lee JR, Lin LY, Shih TH, Stumpp M, Lee MF, et al. Development in a naturally acidified environment: Na<sup>+</sup>/H<sup>+</sup> exchanger 3-based proton secretion leads to CO<sub>2</sub> tolerance in cephalopod embryos. *Front Zool*. 2013; 10:1–16.
- Laurent J, Venn A, Tambutté É, Ganot P, Allemand D, Tambutté S. Regulation of intracellular pH in cnidarians: response to acidosis in *Anemonia viridis*. *FEBS J*. 2014;281:683–95.
- Zoccola D, Tambutté E, Kulhanek E, Puverel S, Scimeca JC, Allemand D, et al. Molecular cloning and localization of a PMCA P-type calcium ATPase from the coral *Stylophora pistillata*. *Biochim Biophys Acta Biomembr*. 2004;1663: 117–26.

42. Barott KL, Venn AA, Perez SO, Tambutteé S, Tresguerres M, Somero GN. Coral host cells acidify symbiotic algal microenvironment to promote photosynthesis. *Proc Natl Acad Sci U S A*. 2015;112:607–12.
43. Decoursey TE. Voltage-gated proton channels and other proton transfer pathways. *Physiol Rev*. 2003;83:475–579.
44. Forgac M. Vacuolar ATPases: rotary proton pumps in physiology and pathophysiology. *Nat Rev Mol Cell Biol*. 2007;8:917–29.
45. Wang Y, Li SJ, Wu X, Che Y, Li Q. Clinicopathological and biological significance of human voltage-gated proton channel Hv1 protein overexpression in breast cancer. *J Biol Chem*. 2012;287:13877–88.
46. Voolstra CR, Li Y, Liew YJ, Baumgarten S, Zoccola D, Flot JF, et al. Comparative analysis of the genomes of *Stylophora pistillata* and *Acropora digitifera* provides evidence for extensive differences between species of corals. *Sci Rep*. 2017;7.
47. Karako-Lampert S, Zoccola D, Salmon-Divon M, Katzenellenbogen M, Tambutté S, Bertucci A, et al. Transcriptome analysis of the scleractinian coral *Stylophora pistillata*. *PLoS One*. 2014;9.
48. Fuster DG, Alexander RT. Traditional and emerging roles for the SLC9 Na<sup>+</sup>/H<sup>+</sup> exchangers. *Pflugers Arch Eur J Physiol*. 2014;466:61–76.
49. Slepokov ER, Chow S, Lemieux MJ, Fliegel L. Proline residues in transmembrane segment IV are critical for activity, expression and targeting of the Na<sup>+</sup>/H<sup>+</sup> exchanger isoform 1. *Biochem J*. 2004;379:31–8.
50. Counillon L, Franchi A, Pouyssegur J. A point mutation of the Na<sup>+</sup>/H<sup>+</sup> exchanger gene (NHE1) and amplification of the mutated allele confer amiloride resistance upon chronic acidosis. *Proc Natl Acad Sci U S A*. 1993; 90:4508–12.
51. Wakabayashi S, Hisamitsu T, Pang T, Shigekawa M. Mutations of Arg440 and Gly455/Gly456 oppositely change pH sensing of Na<sup>+</sup>/H<sup>+</sup> exchanger 1. *J Biol Chem*. 2003;278:11828–35.
52. Holmes RS, Spradling Reeves KD. Evolution of vertebrate solute carrier family 9B genes and proteins (SLC9B): evidence for a marsupial origin for testis specific SLC9B1 from an ancestral vertebrate SLC9B2 gene. *J Phylogenetics Evol Biol*. 2016;4:1–8.
53. Windler F, Bönigk W, Körschen HG, Grahm E, Strünker T, Seifert R, et al. The solute carrier SLC9C1 is a Na<sup>+</sup>/H<sup>+</sup>-exchanger gated by an S4-type voltage-sensor and cyclic-nucleotide binding. *Nat Commun*. 2018;9:1–13. <https://doi.org/10.1038/s41467-018-02523-x>.
54. Smith AN, Finberg K, Wagner CA, Lifton RP, Devonald MAJ, Su Y, et al. Molecular cloning and characterization of Atp6n1b. A novel fourth murine vacuolar H<sup>+</sup>-ATPase  $\alpha$ -subunit gene. *J Biol Chem*. 2001;276:42382–8.
55. Leng XH, Manolson MF, Forgac M. Function of the COOH-terminal domain of Vph1p in activity and assembly of the yeast V-ATPase. *J Biol Chem*. 1998; 273:6717–23.
56. Cotter K, Stransky L, McGuire C, Forgac M. Recent insights into the structure, regulation, and function of the V-ATPases. *Trends Biochem Sci*. 2015;40:611–22. <https://doi.org/10.1016/j.tibs.2015.08.005>.
57. Jr GDS. Cloud thinking - simplifying big data processing. *Target Conf 2013, Probing Big Data answers 2013*;60:195–225.
58. DeCoursey TE. Voltage and pH sensing by the voltage-gated proton channel, H<sub>v</sub>1. *J R Soc Interface*. 2018 Apr;15(141):20180108.
59. Bánfi B, Schrenzel J, Nüsse O, Lew DP, Ligeti E, Krause KH, Demaurex N. A novel H(+) conductance in eosinophils: unique characteristics and absence in chronic granulomatous disease. *J Exp Med*. 1999 Jul 19;190(2):183–94.
60. DeCoursey TE, Cherny WV, Zhou W, Thomas LL. Simultaneous activation of NADPH oxidase-related proton and electron currents in human neutrophils. *Proc Natl Acad Sci U S A*. 2000;97:6885–9.
61. Musset B, Smith SME, Rajan S, Morgan D, Cherny WV, Decoursey TE. Aspartate 112 is the selectivity filter of the human voltage-gated proton channel. *Nature*. 2011;480:273–7. <https://doi.org/10.1038/nature10557>.
62. Capasso M, DeCoursey TE, Dyer MJS. PH regulation and beyond: unanticipated functions for the voltage-gated proton channel, HVCN1. *Trends Cell Biol*. 2011;21:20–8. <https://doi.org/10.1016/j.tcb.2010.09.006>.
63. Stühmer W, Conti F, Suzuki H, Wang X, Noda M, Yahagi N, et al. Structural parts involved in activation and inactivation of the sodium channel. *Nature*. 1989;339:597–603.
64. Ramsey IS, Moran MM, Chong JA, Clapham DE. A voltage-gated proton-selective channel lacking the pore domain. *Nature*. 2006;440: 1213–6.
65. Takeshita K, Sakata S, Yamashita E, Fujiwara Y, Kawanabe A, Kurokawa T, et al. X-ray crystal structure of voltage-gated proton channel. *Nat Struct Mol Biol*. 2014;21:352–7. <https://doi.org/10.1038/nsmb.2783>.
66. Sasaki M, Takagi M, Okamura Y. A voltage sensor-domain protein is a voltage-gated proton channel. *Science*. 2006 Apr 28;312(5773):589–92.
67. Ratanayotha A, Kawai T, Higashijima SI, Okamura Y. Molecular and functional characterization of the voltage-gated proton channel in zebrafish neutrophils. *Physiol Rep*. 2017;5(15):e13345.
68. Rosental B, Kozhekbaeva Z, Fernhoff N, Tsai JM, Traylor-Knowles N. Coral cell separation and isolation by fluorescence-activated cell sorting (FACS). *BMC Cell Biol*. 2017;18:1–12.
69. Ganot P, Zoccola D, Tambutté E, Voolstra CR, Aranda M, Allemand D, et al. Structural molecular components of Septate junctions in cnidarians point to the origin of epithelial junctions in eukaryotes. *Mol Biol Evol*. 2015;32:44–62.
70. Zhao H, Carney KE, Falgout L, Pan JW, Sun D, Zhang Z. Emerging roles of Na<sup>+</sup>/H<sup>+</sup> exchangers in epilepsy and developmental brain disorders. *Prog Neurobiol*. 2016;138–140:19–35. <https://doi.org/10.1016/j.neurobio.2016.02.002>.
71. Watanabe H, Fujisawa T, Holstein TW. Cnidarians and the evolutionary origin of the nervous system. *Develop Growth Differ*. 2009;51:167–83.
72. Furla P, Allemand D, Shick JM, Ferrier-Pagès C, Richier S, Plantivaux A, et al. The symbiotic anthozoan: a physiological chimera between alga and animal. *Integr Comp Biol*. 2005;45:595–604.
73. Saragosti E, Tchernov D, Katsir A, Shaked Y. Extracellular production and degradation of superoxide in the coral *Stylophora pistillata* and cultured symbiodinium. *PLoS One*. 2010;5:1–10.
74. Zhang T, Diaz JM, Brighi C, Parsons RJ, McNally S, Apprill A, et al. Dark production of extracellular superoxide by the coral *Porites astreoides* and representative symbionts. *Front Mar Sci*. 2016;1–16.
75. Raz-Bahat M, Douek J, Moiseeva E, Peters EC, Rinkevich B. The digestive system of the stony coral *Stylophora pistillata*. *Cell Tissue Res*. 2017;368:311–23.
76. Mészáros B, Papp F, Mocsár G, Kókai E, Kovács K, Tajti G, et al. The voltage-gated proton channel hHv1 is functionally expressed in human chorion-derived mesenchymal stem cells. *Sci Rep*. 2020;10:1–16.
77. Harland AD, Brown BE. Metal tolerance in the scleractinian coral *Porites lutea*. *Mar Pollut Bull*. 1989;20:353–7.
78. Reichelt-Brushett AJ, McOrist G. Trace metals in the living and nonliving components of scleractinian corals. *Mar Pollut Bull*. 2003;46:1573–82.
79. Ferrier-Pagès C, Houlbrèque F, Wyse E, Richard C, Allemand D, Boisson F. Bioaccumulation of zinc in the scleractinian coral *Stylophora pistillata*. *Coral Reefs*. 2005;24:636–45.
80. Murphy R, DeCoursey TE. Charge compensation during the phagocyte respiratory burst. *Biochim Biophys Acta Bioenerg*. 2006;1757:996–1011.
81. Venn A, Tambutté E, Holcomb M, Allemand D, Tambutté S. Live tissue imaging shows reef corals elevate pH under their calcifying tissue relative to seawater. *PLoS One*. 2011;6(5):e20013.
82. Taylor AR, Chrachri A, Wheeler G, Goddard H, Brownlee C. A voltage-gated H<sup>+</sup> channel underlying pH homeostasis in calcifying Coccolithophores. *PLoS Biol*. 2011;9:1–14.
83. Lawrence SP, Holman GD, Koumanov F. Translocation of the Na<sup>+</sup>/H<sup>+</sup> exchanger 1 (NHE1) in cardiomyocyte responses to insulin and energy-status signalling. *Biochem J*. 2010;432:515–23.
84. Xia CH, Liu H, Cheung D, Tang F, Chang B, Li M, et al. NHE8 is essential for RPE cell polarity and photoreceptor survival. *Sci Rep*. 2015;5:1–8.
85. Puvarel S, Tambutté E, Zoccola D, Domart-Coulon I, Bouchot A, Lotto S, et al. Antibodies against the organic matrix in scleractinians: a new tool to study coral biomineralization. *Coral Reefs*. 2005;24:149–56.
86. Nishi T, Forgac M. The vacuolar (H<sup>+</sup>)-ATPases - Nature's most versatile proton pumps. *Nat Rev Mol Cell Biol*. 2002;3:94–103.
87. Smith AN, Lovering RC, Futai M, Takeda J, Brown D, Karet FE. Revised nomenclature for mammalian vacuolar-type H<sup>+</sup>-ATPase subunit genes. *Mol Cell*. 2003;12:801–3.
88. Toei M, Saum R, Forgac M. Regulation and isoform function of the V-ATPases. *Biochemistry*. 2010;49:4715–23.
89. Toyomura T, Oka T, Yamaguchi C, Wada Y, Futai M. Three subunit a isoforms of mouse vacuolar H<sup>+</sup>-ATPase. Preferential expression of the  $\alpha$ 3 isoform during osteoclast differentiation. *J Biol Chem*. 2000;275:8760–5.
90. Xiang M, Feng M, Muend S, Rao R. A human Na<sup>+</sup>/H<sup>+</sup> antiporter sharing evolutionary origins with bacterial NhaA may be a candidate gene for essential hypertension. *Proc Natl Acad Sci U S A*. 2007;104:18677–81.
91. Fuster DG, Zhang J, Shi M, Alexandru Bobulescu I, Andersson S, Moe OW. Characterization of the sodium/hydrogen exchanger NHA2. *J Am Soc Nephrol*. 2008;19:1547–56.

92. Holmes R. Evolution of mammalian KELL blood group glycoproteins and genes (KEL): evidence for a marsupial origin from an ancestral M13 type II Endopeptidase gene. *J Phylogenetics Evolutionary Biol.* 2013;01:03. <https://doi.org/10.4172/2329-9002.1000112>.
93. Pedersen SF, Counillon L. The SLC9A-C mammalian Na<sup>+</sup>/H<sup>+</sup> exchanger family: molecules, mechanisms, and physiology. *Physiol Rev.* 2019;99: 2015–113.
94. Liew YJ, Zoccola D, Li Y, Tambutté E, Venn AA, Michell CT, Cui G, Deutekom ES, Kaandorp JA, Voolstra CR, Foret S, Allemand D, Tambutté S, Aranda M. Epigenome-associated phenotypic acclimatization to ocean acidification in a reef-building coral. *Sci Adv.* 2018;4(6):eaar8028.
95. Tambutté E, Venn AA, Holcomb M, Segonds N, Techer N, Zoccola D, et al. Morphological plasticity of the coral skeleton under CO<sub>2</sub>-driven seawater acidification. *Nat Commun.* 2015;6.
96. Guindon S. Bayesian estimation of divergence times from large sequence alignments. *Mol Biol Evol.* 2010;27:1768–81.
97. Darriba D, Taboada GL, Doallo R, Posada D. ProtTest 3: Fasfile:///users/Laura/downloads/gb-2007-8-2-r19.Pdf selection of best-fit models of protein file:///users/Laura/downloads/gb-2007-8-2-r19.Pdf evolution. *Bioinformatics.* 2011;27:1164–5.
98. Bernardet C, Tambutté E, Techer N, Tambutté S, Venn AA. Ion transporter gene expression is linked to the thermal sensitivity of calcification in the reef coral *Stylophora pistillata*. *Sci Rep.* 2019;9:1–13.
99. Hellems J, Mortier G, De Paepe A, Speleman F, Vandensompele J. qBase relative quantification framework and software for management and automated analysis of real-time quantitative PCR data. *Genome Biol.* 2007; 8(2):R19.
100. Zoccola D, Innocenti A, Bertucci A, Tambutté E, Supuran CT, Tambutté S. Coral carbonic anhydrases: regulation by ocean acidification. *Mar Drugs.* 2016;14(6):109. <https://doi.org/10.3390/md14060109>.
101. Moya A, Tambutté S, Bertucci A, Tambutté E, Lotto S, Vullo D, et al. Carbonic anhydrase in the scleractinian coral *Stylophora pistillata*: characterization, localization, and role in biomineralization. *J Biol Chem.* 2008;283:25475–84.

## Publisher's Note

Springer Nature remains neutral with regard to jurisdictional claims in published maps and institutional affiliations.

**Ready to submit your research? Choose BMC and benefit from:**

- fast, convenient online submission
- thorough peer review by experienced researchers in your field
- rapid publication on acceptance
- support for research data, including large and complex data types
- gold Open Access which fosters wider collaboration and increased citations
- maximum visibility for your research: over 100M website views per year

**At BMC, research is always in progress.**

Learn more [biomedcentral.com/submissions](https://biomedcentral.com/submissions)

